Linear Response Domain in Glassy Systems

Stephen R. Williams and Denis J. Evans

Research School of Chemistry, The Australian National University, Canberra ACT 0200, Australia

(Received 30 May 2005; revised manuscript received 13 October 2005; published 6 January 2006)

Molecular dynamics simulations are performed on a realistic glass forming model system. The linear and nonlinear response domains are explored numerically for the case where one of the particles interacts with a constant external force. As the temperature is lowered towards the glass transition, we find that the range of fields over which the response is linear shrinks towards zero. We show that the time required for convergence of the steady state fluctuation theorem and the valid application of the central limit theorem becomes very large as the glass transition is approached. This in turn implies that the domain over which a linear response can be observed becomes progressively smaller.

DOI: 10.1103/PhysRevLett.96.015701 PACS numbers: 64.70.Pf, 05.40.−a, 05.70.Ln

The tagged particle motions of undercooled fluids have been measured in detail, below and approaching the glass transition [1,2]. This tagged particle information may be related to the mobility $\mu(F_e)$ [see Eqs. (2) and (3)] of a particle subject to a constant external force F_e. The mobility in systems approaching the glass transition has been measured directly [3], but in this region it is very difficult to obtain statistically accurate measurements when the force is small enough to observe a linear response $\mu_0 = \mu(0)$. There have been studies of how a system, which is aging after being quenched to a temperature below the glass transition, responds to an external field [4–6]. However, it remains unclear how the region, where a constant external field induces a linear response (the linear domain), behaves as the glass transition is approached. We address this by simulating large ensembles of small systems. This allows the response to be observed for weak fields as well as very close to the glass transition. We use the fluctuation theorem to interpret these results. This study provides new insight into the transition from metastable liquids to amorphous solids.

Our simulations mimic an experiment [3] by using the following time reversible equations of motion for the N-particle system under periodic boundary conditions:

$$\dot{\mathbf{q}}_i = \frac{\mathbf{p}_i}{m}, \qquad \dot{\mathbf{p}}_i = \mathbf{F}_i - \alpha(t)\mathbf{p}_i + s_i F_e \mathbf{i} - \boldsymbol{\gamma}, \tag{1}$$

where $\mathbf{q}_i$ and $\mathbf{p}_i$ are the position and momentum of the ith particle, s_i is a switch set to unity for $i = 1$ and zero otherwise, and F_e is the dissipative external field. We refer to simulations where $F_e \neq 0$ as nonequilibrium molecular dynamics (NEMD). $\boldsymbol{\gamma}$ constrains the total momentum as a constant of the motion, namely, to zero. The term involving $\alpha(t)$ represents a standard Gaussian isokinetic thermostat [7] that models the thermal coupling of the system to a large external heat reservoir.

The steady state nonlinear mobility $\mu(F_e)$, which is even under field reversal and may be represented by an analytic expansion, is defined as

$$\mu(F_e) \equiv \lim_{t\to\infty} \langle \nu_{x1}(t) \rangle / F_e = \mu_0 + \mu_2 F_e^2 + O(F_e^4), \tag{2}$$

where $\langle \nu_{x1}(t) \rangle$ is the ensemble averaged x component of the instantaneous velocity of the particle interacting with the field, at time t. Linear response theory [7] predicts that

$$\lim_{F_e\to 0} \mu(F_e) \equiv \mu_0 \equiv \beta D = \beta \int_0^\infty ds \langle \nu_{x1}(s)\nu_{x1}(0) \rangle_{F_e=0}, \tag{3}$$

where β is the inverse temperature of the heat reservoir and D is the long time self-diffusion coefficient of particle 1. The brackets $\langle \cdots \rangle_{F_e=0}$ denote an equilibrium ensemble average.

The fluctuation theorem (FT) describes a symmetry in the time-averaged fluctuations of the dissipation function (a generalized entropy production) [8,9]. This theorem is extremely general and is valid outside the linear response regime. The transient FT (TFT) quantifies the fluctuations in the response of a system, whose initial ($t = 0$) distribution of phases is known (typically equilibrium). The system responds to the external field $\mathbf{F}_e$ which is switched on at time $t = 0$ [9]. In this case

$$\frac{p(\bar{\nu}_{x1}(t) = A)}{p(\bar{\nu}_{x1}(t) = -A)} = \exp(\beta F_e A t), \tag{4}$$

where $\bar{\nu}_{x1}(t)$ is the time-averaged x velocity of particle $i = 1$ over a time t, $\bar{\nu}_{x1}(t) = \Delta x_1(t)/t$, and $p(\bar{\nu}_{x1}(t) = A)dA$ is the probability of observing $\bar{\nu}_{x1}(t)$ take on a value between $A - dA/2$ and $A + dA/2$. Equation (4) may be partially summed to obtain the integrated transient fluctuation theorem [9],

$$\frac{p(\bar{\nu}_{x1}(t) < 0)}{p(\bar{\nu}_{x1}(t) > 0)} = \langle \exp(-\beta F_e \bar{\nu}_{x1}(t) t) \rangle_{\bar{\nu}_{x1}>0}, \tag{5}$$

where the left-hand side gives the ratio of probabilities of observing trajectories that are, for a time t, in violation of the second law divided by the probability of observing trajectories that are in accord with the second law.

The theory may also be applied asymptotically to the case where $\bar{\nu}_{1t}(t)$ and the resulting probability distributions are measured in a nonequilibrium steady state: the steady state FT (SSFT) [9]. In this case Eqs. (4) and (5) will be

valid in the limit where $t \to \infty$. In equilibrium, $F_e = 0$, the probability, $p(\bar{\nu}_{x1}(t)t) = p(\Delta x_1(t))$, is simply the x component of the self van Hove function, which contains information about the tagged particle motions, equivalent to what can be obtained from a suitable scattering experiment [1,2].

For sufficiently long averaging times we expect that the distribution of time-averaged entropy production should be Gaussian near the mean—a consequence of the central limit theorem (CLT). Recently Evans *et al.* [10] have shown that if the distribution of time-averaged currents is Gaussian near both the mean and the negative of the mean current, and if the system satisfies the SSFT, then

$$\lim_{\substack{t\to\infty \\ F_e^2 t = c}} \langle \nu(t) \rangle = \bar{\nu}_{x1}(t) = \tfrac{1}{2}\beta t \sigma^2_{\bar{\nu}_{x1}(t)} F_e, \tag{6}$$

where the variance is $\sigma^2_{\bar{\nu}_{x1}(t)} = 2D/t$. However, in this long time limit as the averaging time increases, the mean time-averaged velocity and its negative become further and further apart, when measured in units of the standard deviation. For the distribution to remain Gaussian at these two points (i.e., for the CLT to apply near these two points) the field must be decreased as the averaging time is increased; hence the double limit appearing in Eq. (6) [10]. Combining Eq. (6) with Eq. (2) leads directly [10] to the linear response result, namely, Eq. (3) [10]. The external field value given in (6) is the *largest* possible field value for which the resultant Green-Kubo relations (i.e., linear response) can be expected to apply. For the particular case here the condition that the mean $\langle \bar{\nu}_{x1}(t) \rangle = \beta D F_e$ divided by the standard deviation $\sigma_{\bar{\nu}_{x1}(t)}$ remains constant results in the maximum force scaling as $F_{\rm em} \propto k_B T/\sqrt{D t_c}$ where t_c is the shortest time for which both the SSFT has converged and the CLT is valid.

All simulations are three-dimensional. Our model is similar to the Kob and Andersen potential [2] except we use a shifted cutoff radius of $2^{1/6}\sigma_{\alpha\beta}$ and set $\varepsilon_{AB} = 0.96$ and $\varepsilon_{BB} = 0.387$. The system consists of 108 particles with the first 86 being of species A and the remaining 22 being of species B to form an 80%:20% mixture. The number density is $\rho = N\sigma^3_{AA}/V = 1.2$, the time unit is $\sqrt{m\sigma^2_{AA}/\varepsilon_{AA}}$, and the temperature T unit is ε_{AA}/k_B. Only particle $i = 1$ interacts with the external field F_e. Long time self-diffusion coefficients Eq. (3) were obtained from equilibrium simulations $F_e = 0$, at temperatures above the glass transition temperature T_g and may be seen on a logarithmic plot in Fig. 1. Using the mode-coupling asymptotic scaling prediction for the self-diffusion coefficient $D \propto (T - T_g)^b$, we obtain values of $T_g \approx 0.42$, $b \approx 0.9$. This allows a comparison with other work where this method has been used [1,2]. The glass transition temperature thus obtained is significantly affected by the small size of the system. For large systems using this potential it may be necessary to slightly increase the density to observe a glass transition.

We set up a series of simulations with various values for the temperature T and the field strength F_e. For each state point in this series 10^5 steady state trajectory segments were simulated to allow the distribution functions $p(\Delta x_1(t))$ to be constructed.

In the linear regime the zero field mobility was determined using Eq. (3). The field dependent mobilities were obtained from NEMD simulations using Eq. (2). The results are summarized in Table I along with the long time self-diffusion coefficients Eq. (3). These mobilities have been calculated with high accuracy due to the very large amount of statistical sampling in the 10^5 member NEMD ensembles and have allowed us to observe a linear response very close to the glass transition temperature. Also shown are estimates of the field strength where the relative nonlinear component of the mobility reaches 1%, $\mu(F_{em})/\mu_0 = 1.01$, using the leading order expansion Eq. (2).

At the highest temperature $T = 5$ the response is linear within the statistical error, for all field strengths shown. As the temperature is lowered, a significant and increasing field strength dependence is observed. For the temperature of $T = 0.425$ we observe a significant field dependence for the three different field strengths studied by NEMD. If we make the field strength very small, the response becomes too weak to measure amid the background statistical noise.

TABLE I. The first column gives the temperature studied, the second gives the duration of the NEMD simulations, and the third gives the equilibrium diffusion coefficient for species A particles. The fourth column is the mobility calculated using linear response theory, Eq. (3). The next three columns are the mobilities obtained at various external field strengths F_e from the NEMD simulations using Eq. (2). The single figures in the parentheses are the error margins in the least significant figure shown. For the temperature $T = 0.425$ these were estimated *ad hoc,* otherwise set to 2 standard errors. The final column shows the external force for which the relative nonlinear component of the mobility reaches 1% estimated using Eq. (2), $F_{\rm em} = \sqrt{0.01\mu_0/\mu_2}$. For the temperatures of $T = 1$ and above, higher field strengths than those shown in the table were used to estimate μ_2.

k_BT	Duration	D	$\mu(0)$	$\mu(1)$	$\mu(2)$	$\mu(4)$	$F_{\rm em}$, 1%
5	40	0.157	0.0315	⋯	0.0316(4)	0.0314(2)	27
2	40	0.0491	0.0246	⋯	0.0246(1)	0.0247(1)	7.1
1	40	0.0152	0.0152	⋯	0.0155(1)	0.015 77(4)	2.6
0.5	80	0.002 44	0.004 88	0.004 90(4)	0.005 03(3)	0.005 60(2)	1.0
0.45	180	0.0012	0.0027(5)	0.0027(3)	0.0028(3)	0.0035(3)	0.7
0.425	180	0.0002	0.0005(5)	0.0006(1)	0.0010(2)	0.0016(2)	0.3

The dramatic dynamical slowing, as the temperature is cooled towards the glass transition, further compounds this difficulty.

We now turn our attention to the distribution functions $p(\Delta x_1)$ for times given in the duration column of Table I. Figure 2(a) shows the distribution functions at various field strengths at the temperature $T = 5.0$. We see these are all similar Gaussian distributions, differing only in their mean, as is required for Eq. (3) to hold. At these field strengths the mobility is also independent of the field indicating that the response is linear. In Fig. 2(b) we see very different distribution functions for the slow glassy dynamics $T = 0.45$. We also see that the distribution functions change with increasing field strengths. At this low temperature a significant number of the trajectory segments appear to have zero mobility in the steady state, and thus we observe a sharp peak, centered on zero with constant variance, for all field strengths studied. This is in accord with the observation of dynamic heterogeneities for glassy systems with no applied external field [11–13]. This effect becomes more dramatic for the temperature of $T = 0.425$ which is not shown. These dynamical heterogeneities show that the shortest time for which the CLT may be applied grows dramatically as the glass transition is approached. If this time diverges rapidly enough, it will be responsible for the reduction in the maximum field strength F_{em} by the scaling argument from the SSFT discussed above.

In Figs. 3 and 4 we present the results of applying the FT [Eq. (4)] to the NEMD simulations. In Fig. 3 we test the steady state integrated FT (SSIFT) at different field strengths and temperatures. At $T = 5$ the SSIFT is clearly satisfied for all times displayed in the figure. As the temperature is progressively lowered, the asymptotic SSIFT takes longer to converge, but at sufficiently long times it seems it will converge. This convergence time is also sensitive to the external field strength. As the field strength is lowered the convergence time increases. From our data it is not possible to determine whether the linear domain is shrinking due to the SSFT convergence time diverging or due to the time the CLT converges on diverging (dynamic heterogeneities) as the glass transition temperature is approached. However, in Fig. 1 we see the ratio of the coefficients from Eq. (2), μ_0/μ_2, scales very closely with the diffusion coefficient as the glass transition is approached. This means the maximum field strength for a linear response scales as $F_{\mathrm{em}} \propto \sqrt{D}$ upon approaching the glass transition. At the glass transition the linear response regime shrinks to zero. Consideration of growing length scales may result in similar conclusions [14].

Figure 4 shows the distinct SSFT for a range of temperatures. At the highest of these temperatures the SSFT is satisfied at the time of $t = 80$. At $T = 0.45$, 0.425, and $t = 180$ we are unable to verify the SSFT consistent with the results in Fig. 3. At the lowest temperature $T = 0.425$ where the convergence time for the SSFT is expected to be the slowest, the TFT (upon which the SSFT is predicated) is satisfied—see Fig. 4. The standard arguments that

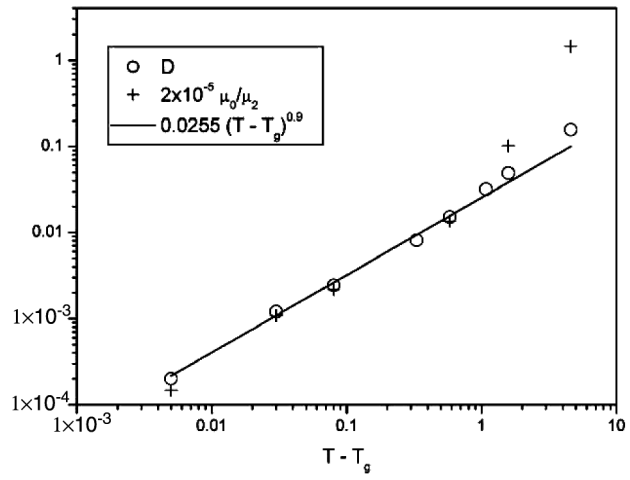

FIG. 1. A log-log plot of the diffusion coefficient D for the species A particles and μ_0/μ_2 versus $T - T_g$ where $T_g = 0.42$. The asymptotic scaling fit is also shown. The plot makes it clear that the maximum force for a linear response scales as $F_{\mathrm{em}} \propto \sqrt{D}$ upon approaching the glass transition.

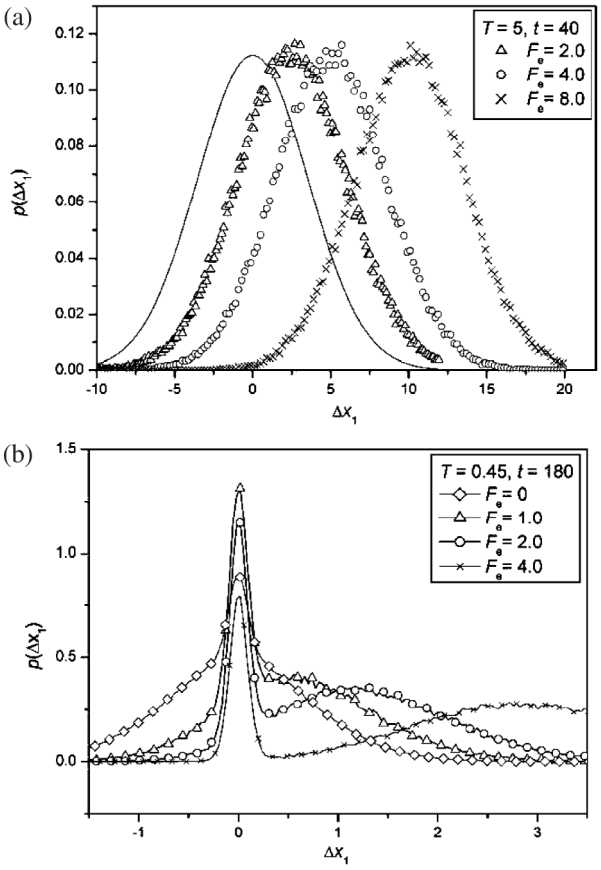

FIG. 2. Distribution functions for the response of the particle $\Delta x_1(t)$ to the external field of various strengths at the time t and temperature T given in the legend. The solid line in (a) is a zero mean Gaussian with its variance determined using the appropriate diffusion coefficient from Table I.

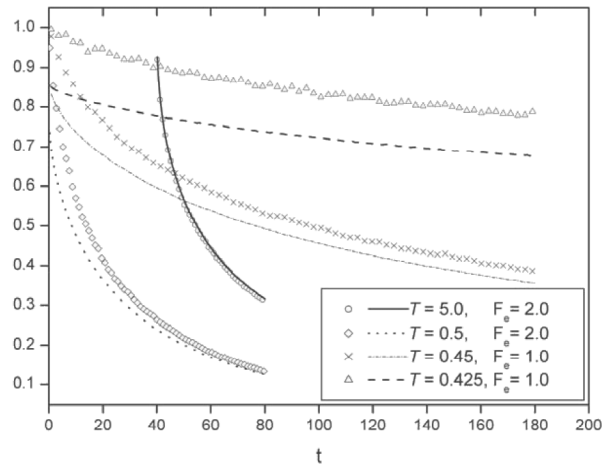

FIG. 3. Steady state fluctuation theorem results for various temperatures. The plots make use of the integrated fluctuation theorem Eq. (5). The symbols are the ratio $p[\Delta x_1(t) < 0]/p[\Delta x_1(t) > 0]$ while the lines are the function $\langle \exp(-\beta F_e \Delta x_1(t)) \rangle_{\Delta x > 0}$. It is important to note that the $T = 5$ data have been shifted 40 units forward along the time axis for clarity.

are used to prove the SSFT from the TFT would seem to imply that if the TFT is satisfied for arbitrary averaging times then in the long time limit the SSFT must also be valid—see Ref. [9]. If the TFT is valid for arbitrary averaging times, even at the lowest temperature without employing an effective temperature [15], then there is no doubt that in the absence of an external field all our systems may be treated as having equilibrated. Figures 3 and 4 suggest that both fluctuation theorems (steady state and transient) are valid for glass forming fluids for temperature quenches that are deep and go quite close to the glass transition temperature.

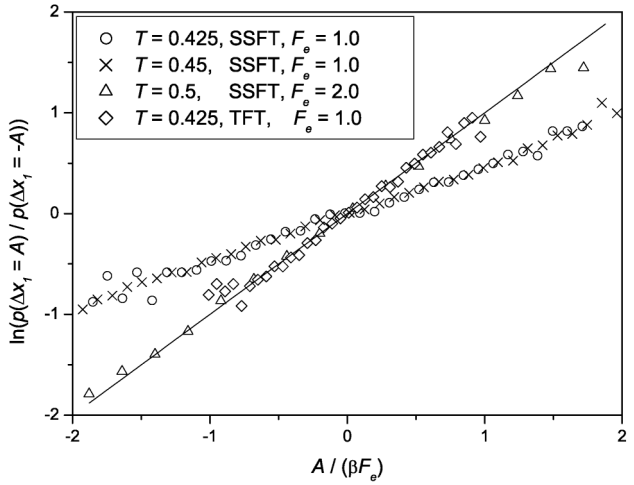

FIG. 4. Fluctuation theorem plots. Shown are the steady state theory (SSFT) at temperatures of $T = 0.5$, 0.45, and 0.425 calculated at times of $t = 80$, 180, and 180, respectively. The solid line is the prediction of the theory. While strong agreement is observed for $T = 0.5$, this is not the case for $T = 0.45$ and 0.425 due to a slower asymptotic convergence. The transient theory (TFT) data for $T = 0.425$ at a time of $t = 30$ is also shown and is consistent with the theory.

We have provided convincing evidence that the transient fluctuation theorem holds for glassy systems. We have presented simulation data and theoretical arguments that the steady state fluctuation theorem also holds for these systems; however, our data suggest that as the glass transition is approached, the time for the asymptotic SSFT to converge becomes very large indeed, diverging to infinity at the glass transition itself. Recent theoretical results [10] show that if this convergence time for the SSFT or the CLT diverges to infinity as the glass transition is approached, then the domain of linear response must shrink to zero. At the glass transition itself the steady state response to a constant applied field on a test particle is intrinsically nonlinear. Below the glass transition the zero field mobility is zero $\mu_0 = 0$ and to leading order we expect to observe $\langle \nu_{x1}(t) \rangle = \mu_2 F_e^3 + O(F_e^5)$ in the steady state. Our model exhibits finite size effects, but we expect they are merely quantitative and have no bearing on the conclusions reached.

We thank the Australian Research Council for financial support and the Australian Partnership for Advanced Computing for computational facilities. Debra J. Searles, Bill van Megen, and Willem Kegel are thanked for helpful discussions.

[1] W. van Megen, T. C. Mortensen, S. R. Williams, and J. Muller, Phys. Rev. E **58**, 6073 (1998).
[2] W. Kob and H. C. Andersen, Phys. Rev. E **51**, 4626 (1995).
[3] P. Habdas, D. Schaar, A. C. Levitt, and E. R. Weeks, Europhys. Lett. **67**, 477 (2004).
[4] G. Parisi, Phys. Rev. Lett. **79**, 3660 (1997).
[5] J.-L. Barrat and W. Kob, Europhys. Lett. **46**, 637 (1999).
[6] B. Abou and F. Gallet, Phys. Rev. Lett. **93**, 160603 (2004).
[7] D. J. Evans and G. P. Morriss, *Statistical Mechanics of Nonequilibrium Liquids* (Academic, London, 1990); also available at http://rsc.anu.edu.au/~evans/evansmorrissbook.htm
[8] D. J. Evans, E. G. D. Cohen, and G. P. Morriss, Phys. Rev. Lett. **71**, 2401 (1993).
[9] D. J. Evans and D. J. Searles, Adv. Phys. **51**, 1529 (2002).
[10] D. J. Evans, D. J. Searles, and L. Rondoni, Phys. Rev. E **71**, 056120 (2005).
[11] W. K. Kegel and A. van Blaaderen, Science **287**, 290 (2000).
[12] W. van Megen, J. Phys. Condens. Matter **14**, 7699 (2002).
[13] M. M. Hurley and P. Harrowell, Phys. Rev. E **52**, 1694 (1995).
[14] J. P. Bouchaud and G. Biroli, cond-mat/0501668.
[15] F. Zamponi, G. Ruocco, and L. Angelani, Phys. Rev. E **71**, 020101 (2005).